ACS APPLIED MATERIALS & INTERFACES

Research Article

www.acsami.org

Transparent and Hard Zirconia-Based Hybrid Coatings with Excellent Dynamic/Thermoresponsive Oleophobicity, Thermal Durability, and Hydrolytic Stability

Benjamin Masheder, Chihiro Urata, and Atsushi Hozumi*

National Institute for Advanced Industrial Science and Technology (AIST), 2266-98, Anagahora, Shimo-shidami, Moriyama-ku Nagoya 463-8560, Japan

Supporting Information

ABSTRACT: Smooth, transparent, and extremely hard zirconia (ZrO_2)-based inorganic−organic hybrid films showing excellent dynamic oleophobicity, thermal durability, and hydrolytic stability were successfully prepared through a simple combination of zirconium tetrapropoxide ($Zr(O(CH_2)_2CH_3)_4$) with stearic acids. In this study, we have particularly focused on the effects of stearic acid molecular architecture (linear-stearic acid (LSA) and branched-stearic acid (BSA)) on surface physical/chemical properties. Although, in each case, the resulting hybrid (Zr:LSA and Zr:BSA) films achieved by a simple spin-coating method were highly smooth and transparent, the final surface properties were markedly dependent on their molecular architectures. Thanks to the thermal stability of BSA, our Zr:BSA hybrid films displayed a greatly improved thermal effective range (maximum of 200 °C), while for Zr:LSA hybrid films, serious thermal damage to surface dewetting behavior was observed at less than 150 °C. The hardness of the Zr:BSA hybrid films were markedly increased by curing at 200 °C for 1 h (from 1.95 GPa to 3.03 GPa), while maintaining their dynamic dewettability toward *n*-hexadecane, when compared with Zr:LSA hybrid films (0.95−1.19 GPa). Small volume *n*-hexadecane droplets (5 μL) were easily set in motion, sliding across and off our best Zr:BSA hybrid film surfaces at low substrate tilt angles (<10°) without pinning. Moreover, they also showed thermoresponsive dynamic dewetting behavior, reasonable resistance to hydrolysis in an aqueous environment, and antifingerprint properties.

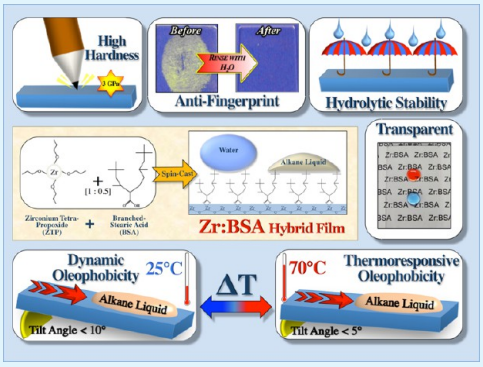

KEYWORDS: *zirconia-based hybrid film, branched-stearic acid, dynamic oleophobicity, hardness, thermal durability, hydrolytic stability*

INTRODUCTION

The creation of synthetic surfaces that easily dewet various organic liquids—in particular, low surface tension liquids such as alkanes (nonpolar) and alcohols (polar)—from their surfaces has attracted great attention lately.[1−9] Extensive research into the preparation of superhydrophobic (contact angle (CA) of >150°) surfaces, with low CA hysteresis (where CA hysteresis ($\Delta\theta$) = advancing (θ_A) − receding (θ_R) CA, <5°) and/or substrate tilt angles (substrate TAs, <10°) for water droplets several microliters in volume have been reported over the past decade.[10−15] In comparison, there have been far fewer papers reporting superoleophobic surfaces demonstrating CA > 150°, $\Delta\theta$ < 5°, and/or substrate TA < 10° for microliter-scale organic liquid droplets with low surface tension.[1,2,4,6,8] To achieve such superoleophobic surfaces, established techniques for preparing superhydrophobic surfaces, which have relied mainly on surface roughening and subsequent perfluorination using long-chain perfluorinated compounds (LCPFCs) to reduce contact area and increase static CAs (θ_S), have been generally employed.[16−18] However, most of them have proved less effective at dewetting organic liquids, which tend to pin to the surfaces or require much higher substrate TAs, because of their low surface tension.[19,20] Only specifically structured surfaces prepared using re-entrant curved micropatterns/nanopatterns,[1,2] electrospun[1,2,8] or self-assembled nanofilaments,[4] and candle-soot layers[6] coated with LCPFCs have met the severe demands for the superoleophobic surfaces described above. However, preparation of such textured surfaces is rather complicated, consisting of a sequence of many processes, hampering practical applications. Such roughened surfaces also possess poor optical properties and lack resistance to physical abrasion, leading to a reduction in the ability to dewet liquids. Although efforts are being made to increase the durability or reduce the effects of surface damage on the dewettability of such surfaces, a solution still remains distant.[21] In addition to these shortcomings, there have been concerns raised about the effects of LCPFCs on human health and the environment. Some LCPFCs commonly used for dewettable coatings have recently been listed as persistent organic pollutants.[22,23] Hence, an alternative oleophobic

Received: May 24, 2013
Accepted: July 12, 2013
Published: July 12, 2013

   dx.doi.org/10.1021/am401992h | ACS Appl. Mater. Interfaces 2013, 5, 7899−7905

dewettable coating method requiring neither surface roughening nor subsequent perfluorination has been strongly demanded.

In contrast to such conventional approaches, studies on the formation of smooth liquid-repellent surfaces have been rarely seen. Wong et al.[3] and Ma et al.[24] recently reported smooth liquid surfaces showing excellent dynamic dewetting behavior toward various probe liquids through the entrapment of immiscible liquids on porous/textured surfaces. They employed nano/microstructured substrates infused with thick noncovalently bound films of lubricating perfluorinated fluids. However, such lubricating liquid films, while promising, must be easily contaminated by impurities and applicable only under determinate conditions. Our group and McCarthy's group have demonstrated in several publications that comparable or better dewettability toward various nonpolar liquids could be achieved using many smooth surfaces containing specifically featured monolayers,[25−28] low-molecular weight poly(dimethylsiloxane) (PDMS) polymer brushes,[5,7,29] and alkylsilane-derived sol−gel hybrid films.[30,31] These nonperfluorinated smooth surfaces appear statically oleophilic (θ_S < 30°), but dynamically oleophobic, where small volume organic liquid drops easily move and need only low substrate TAs (<10°) to roll off in all cases. A common feature among these highly dynamically oleophobic surfaces is the fact that functional groups in the surface-tethered molecules are highly mobile and as a result the physical nature of such a surface is considered to be liquid-like, and that droplets in contact with them experience very low energy barriers between metastable states, leading to the formation of low $\Delta\theta$ surfaces.[32−34] These approaches to dewettability are conceptually distinct from conventional approaches, because they have not focused on CA magnitude but on the control of $\Delta\theta$ (generally, <5°). However, the practical applicability of such surfaces is intrinsically limited, because these monomeric layers and polymer brush films are inevitably very thin (0.5−8.0 nm).[5,7,25−29] Consequently, the final surface wettability is markedly influenced by the substrate surface roughness and morphology. Although, sol−gel films are sufficiently thick (typically more than 250 nm) to eliminate the influence of substrate roughness, unfortunately, the mechanical and thermal robustness of these smooth dewettable films presently are still insufficient.[9,30,31,35] Thus, the next level of accomplishment in this research area remains the further development of new liquid-like surfaces possessing enhanced physical properties, such as high hardness and thermal durability.

In an effort to address these challenges, we began to study sol−gel hybrid films based on zirconia (ZrO_2)-containing components, because ZrO_2 is well-known for its high transparency and mechanical/chemical durability, making it potentially ideal for practical applications. In our previous study, we demonstrated that ZrO_2 sol−gel hybrid films containing linear-fatty acids having various alkyl chain lengths (carbon numbers of 10−24) displayed excellent transparency and dynamic/thermal responsive dewettability against alkane liquids.[35] However, because of the high organic content and the poor thermal stability of the incorporated organic molecules, the resulting hybrid film possessed a maximum hardness of only 0.2 GPa and a low heat resistance (limited to 100 °C for 1 h).[35]

To overcome these shortcomings, we have particularly focused on highly branched fatty acids, because they are known to have a higher thermal stability than their linear isomers, as a consequence of the effects of protobranching and greater delocalization of electrons in their structures.[36] Upon creation of new hybrid films using such specific-featured molecules, we found that a significant reduction in the organic content of the hybrid films (reduced by 50%, compared to our previous ZrO_2−stearic acid hybrid films[35]) could be achieved without inhibiting oleophobic dewetting. As a result, the density of the surface-tethered functional groups was reduced, allowing them the increased freedom to move and act in a liquid-like manner. Similarly, thanks to the presence of the thermally stable branched molecules and lower organic concentration, we could cure the resultant films at relatively high temperatures (200 °C) without degrading surface dewettability. Moreover, such high-temperature treatment greatly contributed to an enhancement of the hybrid film hardness. By selecting a highly branched-stearic acid and adjusting appropriate conditions, we successfully prepared ZrO_2-based sol−gel hybrid films that displayed not only outstanding transparency and dynamic oleophobicity but also significantly improved hardness, thermal durability, and hydrolytic stability. Furthermore, our hybrid films demonstrated excellent antifingerprint properties.

EXPERIMENTAL SECTION

Materials. Branched-stearic acid (BSA, FINEOXOCOL) was given as a gift from Nissan Chemical America Corporation. Zirconium tetrapropoxide (70 wt %) in isopropanol ($Zr(O(CH_2)_2CH_3)_4$, abbreviated as ZTP) and glacial acetic acid were purchased from Tokyo Chemical Industries Co., Ltd. (Tokyo, Japan). Isopropanol (IPA) and linear-stearic acid (LSA) were purchased from Wako Pure Chemical Industries, Ltd. (Osaka, Japan). All chemicals were used as-received, without further purification.

Precursor and Hybrid Film Preparation. The sol−gel precursors were prepared according to our previous report.[35] ZTP (1 mL) was first combined with BSA (0.28 g) at a molar ratio of 1: 0.5 in a dry N_2 atmosphere to produce $[Zr(O(CH_2)_2CH_3)_{3.5}(C_{18}H_{36}O_2)_{0.5}]$. After vigorous stirring for 10 min at 80 °C, the open vial was placed into a 60 cm^3 Teflon container in a dry N_2 atmosphere. The container was sealed with a cap and then heated for 12 h in an oven maintained at 150 °C. Because of this treatment, a transparent and stable inorganic−organic hybrid precursor was achieved, hereafter referenced as Zr:BSA. Upon removal from the oven, the vial was sealed and then placed in an oven maintained at 70 °C until it was used. Finally, glacial acetic acid (0.20 mL) was added to the Zr:BSA precursor with stirring on a hot plate kept at 80 °C. After 20 s, IPA (20 mL) was added and stirred for another minute. The mixture was then spin-cast (at 1000 rpm for 5 s, then 2000 rpm for 20 s) onto UV/ozone-cleaned glass slides (28 mm × 48 mm) and Si substrates covered with native oxide (SiO_2/Si, 15 mm × 15 mm). During spin coating, the substrates were maintained at ∼60 °C. After coating, the samples were dried at 25 °C for 1 h and then cured at 100, 150, or 200 °C for 1 h before characterization. As a control experiment, hybrid films containing linear-stearic acid (LSA) were prepared under the same conditions. We hereafter refer to this precursor as Zr:LSA.

Characterization. CAs and substrate TAs were measured with a CA goniometer (Kyowa Interface Science, Dropmaster DM-500). The static (θ_S), advancing (θ_A), and receding (θ_R) CAs were collected using Milli-Q water (10^{-15} Ω/cm) and *n*-hexadecane as probe liquids at room temperature (25 °C). The θ_S values were measured by gently placing a drop of the probe liquid (∼3 μL) on the horizontal surface. For θ_A and θ_R measurements, probe liquid droplets (∼3 μL) were added and withdrawn from the surface, respectively. CAs were gathered at five different locations on three separately prepared surfaces and the θ_S, θ_A, and θ_R reported are the averages of the values gathered. All measurements were taken under ambient conditions, unless otherwise stated; values for each sample were in the range of ±2°. The CA hysteresis ($\Delta\theta = \theta_A - \theta_R$ and $\Delta\theta_{cos} = \cos\theta_R - \cos\theta_A$)

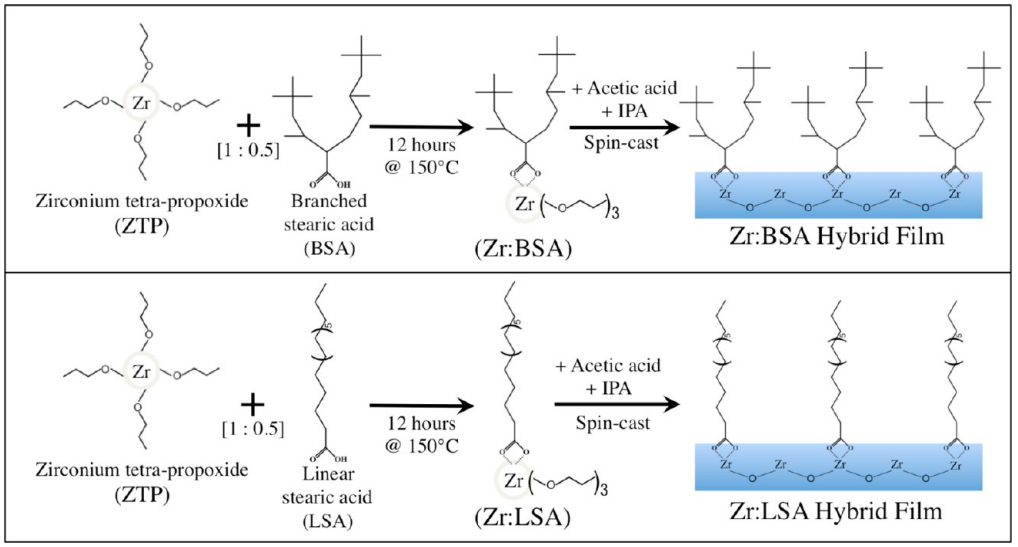

Figure 1. Schematic illustration showing the synthetic steps taken during the formation of Zr:BSA (top) and Zr:LSA (bottom) hybrid films.

were calculated using dynamic CA data.[7] The minimum substrate TA required to set a droplet of water (60 μL) or *n*-hexadecane (5 μL) in motion was measured and taken as an average of at least five measurements at different locations on three separately prepared samples. The optical transparency of our hybrid films in the visible range (400−800 nm) was measured by UV−vis spectroscopy (Agilent Technologies, Cary 5000 UV-vis-NIR spectrometer). The morphology of the samples was observed by both atomic force microscopy (AFM) (Park Systems, Model XE-100) with a Si probe in tapping mode (Park Systems, Model 910M-NCHR; spring constant = 42 N/m and response frequency = 330 kHz) and field-emission scanning electron microscopy (FE-SEM) (JEOL, Model JSM-7100F). The indentation hardness of the samples was measured using an automated dynamic-ultramicrohardness tester (Shimadzu, Model DUH-201) with a Vickers indenter. Loading and unloading tests were preformed with an indentation load of 1 mN at a rate of 0.14 mN s^{-1}, the dynamic hardness was estimated from the depth of the indentation as a result of plastic deformation. All hardness data were normalized by the dynamic hardness of soda−lime glass (5.5 GPa); the reported hardnesses were an average of five measurements. The adhesion strength between the hybrid film and the substrate was evaluated based on a standard cellophane (3M Scotch tape) peeling test.[37,38] A cross-cut area of the hybrid film was covered with cellophane (3M Scotch tape) that was applied with moderate pressure. After 30 s, the tape was removed quickly from the substrate. This test was repeated at least 10 times. Hydrolytic stability of our hybrid films was investigated as follows. Each substrate was immersed in hot Milli-Q water (100 mL, 90 °C, neutral pH) for the designated times (2, 5, 15, 25, 45, and 60 min). After immersion, the samples were removed from the water, rinsed thoroughly with additional Milli-Q water, and then dried in a dry N_2 gas atmosphere. Changes in surface properties were monitored using water and *n*-hexadecane CA measurements. Human fingerprints were applied to our hybrid films and a bare glass slide (control) with a consistent pressure (~0.16 kg/cm^2) for 5 s. Water was then flowed over the fingerprints for 20 s. Fluorescent fingerprint powders were employed to detect remaining fingerprints on both surfaces before and after washing with water.

RESULTS AND DISCUSSION

Hybrid Film Formation. Figure 1 shows a schematic illustration of our experimental procedure. All precursor solutions, that is, Zr:BSA and Zr:LSA (the latter serving as a control), were highly transparent. Upon spin coating, both hybrid films were successfully formed on glass slides and Si wafers. The average film thickness of Zr:BSA and Zr:LSA hybrid films measured by a stylus profiler was ~340 and 300 nm, respectively. As shown in Figure 2, the as-prepared Zr:BSA

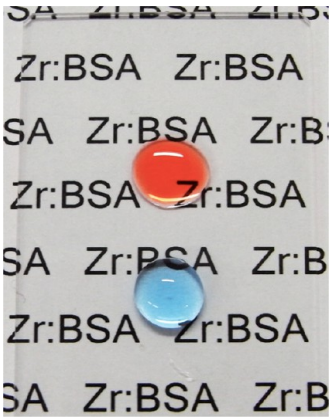

Figure 2. Optical photograph of *n*-hexadecane (red) and water (blue) droplets on our Zr:BSA-hybrid film-covered glass slide.

hybrid film was highly transparent and colorless, the characters behind the sample clearly visible. In fact, the transmittance of this hybrid film-coated glass slide in the visible-light wavelength range (400−800 nm) was almost the same as that of the uncoated glass slide (over 90%). (See Supporting Information, Figure S-1.) As shown in Figure 3, an AFM image of a Zr:BSA hybrid film cured at 100 °C for 1 h revealed a highly smooth and defect-free surface at a short length scale. The average root-mean-square roughness (R_{rms}) of the sample was estimated to be 0.280 nm from the AFM image (3 μm × 3 μm). FE-SEM observation of an identical sample also demonstrated a flat surface at a larger length scale that contained no aggregates, defects, or additional topography over the entire substrate. (See Supporting Information, Figure S-2.) There were no marked differences in surface morphologies for all samples before and after curing. Our Zr:BSA hybrid surfaces appeared to be similar to that of the cleaned SiO_2/Si substrate (image not shown, R_{rms} ≈ 0.2 nm). Thus, surface morphology has little, if any, influence on the dewettability differences of sample surfaces. Furthermore, this Zr:BSA hybrid film showed exceptional adhesion to glass slides and SiO_2/Si substrates, independent of the film

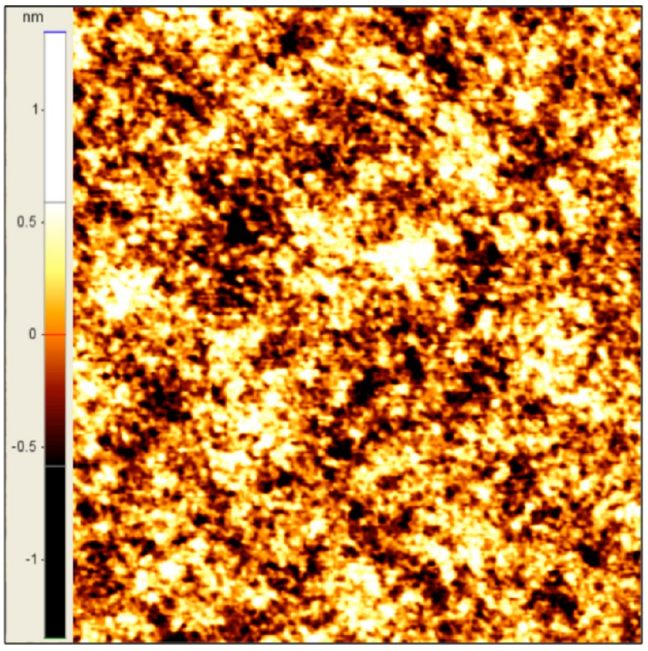

Figure 3. Typical AFM image (3 μm × 3 μm) of a Zr:BSA hybrid film cured at 100 °C for 1 h. The root-mean-square roughness (R_{rms}) was estimated from this image to be 0.280 nm.

thickness or curing conditions. No peeling of the films was observed in a cellophane (3M Scotch tape) peeling test. Zr:LSA hybrid films also showed almost identical film properties. There were no marked differences in optical properties, surface morphologies, and adhesion strength between the Zr:BSA and Zr:LSA hybrid films.

Dynamic Dewettability of Hybrid Films. Next, we investigated surface dewettability (including θ_S, θ_A/θ_R, $\Delta\theta$, $\Delta\theta_{cos}$, and substrate TA) of our hybrid films (cured at 100 °C for 1 h) toward various probe liquids. The results are summarized in Table 1. Unfortunately, we could not obtain

Table 1. Static (θ_S) and Dynamic Dewettability (θ_A/θ_R, $\Delta\theta$, $\Delta\theta_{cos}$, and Substrate TA) of Water and *n*-Hexadecane Droplets on Zr:BSA and Zr:LSA Hybrid Films

probe liquid	θ_S (°)	θ_A/θ_R (°)	$\Delta\theta$ (°)	$\Delta\theta_{cos}$ (−)	TA (°)
		Zr:BSA Hybrid Film			
H_2O	98.9	106.8/77.6	29.2	0.505	68.0[a]
n-hexadecane	23.9	26.0/21.1	4.9	0.034	10.4
		Zr:LSA Hybrid Film			
H_2O	105.6	111.0/93.6	17.4	0.296	35.0[a]
n-hexadecane	20.6	24.9/16.0	8.9	0.054	11.4

[a]60 μL droplets of water were used during substrate TA measurements.

CA data using *n*-dodecane and *n*-decane, because they completely wet our Zr:BSA hybrid film. Thus, water and *n*-hexadecane were employed for the measurements that follow. Both Zr:BSA and Zr:LSA hybrid films were hydrophobic and oleophilic in static situations, 98.9° < θ_S < 105.6° for water, and 20.6° < θ_S < 23.9° for *n*-hexadecane. However, despite such low static CAs, our Zr:BSA hybrid film could easily dewet *n*-hexadecane in a dynamic situation. Thanks to low CA hysteresis (θ_A/θ_R = 26.0°/21.1°, $\Delta\theta$ = 4.9°, $\Delta\theta_{cos}$ = 0.034), small volume droplets (5 μL) of *n*-hexadecane slide off the Zr:BSA hybrid film surface at substrate TAs as little as 9.0° (see Supporting Information, Movie S-3). Such excellent dewettability of *n*-hexadecane is comparable to other alkylsilane-derived sol−gel hybrid films (substrate TAs < 10°).[30,31] On the other hand, in the case of water, the $\Delta\theta$ and substrate TA values on both hybrid film surfaces were considerably large, compared to *n*-hexadecane. Such inferior dynamic dewettability for water has been frequently observed in other coated/grafted surfaces.[5,7,9,30,31,35,39,40] In such cases, a mutual interaction between surface residual polar functional groups (in the present case, Zr−OH) and water[39,40] must be the origin of the strong adhesion (pinning) observed on both hybrid surfaces.

It is noteworthy that substrate TAs of *n*-hexadecane for Zr:BSA and Zr:LSA hybrid films cured at 100 °C for 1 h, shown in Table 1, were almost identical (10.4° and 11.4°, respectively), despite the different molecular architecture of the stearic acids. This clearly indicates that the surface properties of Zr:BSA hybrid films are similar to those of the Zr:LSA hybrid films. Because of effective reduction of functional group packing density either through the control of composition of binary mixtures (ZTP and LSA) or use of specific-featured molecules (BSA), both hybrid surfaces exhibited liquid-like natures with lower $\Delta\theta$ values, resulting from the high mobility of functional groups in the surface-tethered molecules. This contributes to a low resistance to probe liquid droplet motion and low energy barriers between metastable states.[32−34] We believe that these liquid-like properties may help to form the oleophobic surfaces, showing unusual dynamic CA behavior toward *n*-hexadecane. However, the different architecture of the isomers, specifically the enhanced stability of the BSA molecules, produced clear differences in the final surface physical/chemical properties of the hybrid films when the curing temperatures were increased to 200 °C. We will discuss these in the next section.

Hardness of Hybrid Films. Because of the excellent thermal stability of the BSA molecule, we were able to cure the Zr:BSA hybrid film at a high temperature (200 °C). Such high-temperature treatment greatly enhanced the hardness of the Zr:BSA-derived hybrid film. In the present case, the maximum hardness (3.03 GPa) was achieved when the film was cured at 200 °C for 1 h, which is comparable to that of pure amorphous ZrO_2 films prepared via the sol−gel method (~3 GPa, curing temperature was 400 °C).[41] Moreover, this value is significantly higher than any previous reported values for transparent oleophobic coatings prepared via the sol−gel method (polysiloxane coating, 0.8−1.5 GPa, curing temperature = 150−400 °C).[42] However, when the curing time was extended up to 24 h, hardness of the Zr:BSA hybrid film was further increased but significant degradation of dewettability was observed. On the other hand, the Zr:LSA hybrid film surface became irreversibly wetted after curing at 150 °C for 24 h and 200 °C for 1 h, as a result of thermal damage to the LSA molecules. Thus, curing at 150 °C for 1 h was considered to be the limit for the Zr:LSA hybrid film. In this case, the maximum hardness of the Zr:LSA hybrid film was estimated to be only 1.19 GPa. As shown in Table 2, in the case of Zr:BSA-derived hybrid films, even under lower curing conditions (at 100 and 150 °C), their average hardness was ~2 times higher than those of the Zr:LSA hybrid films cured under the same conditions. Dynamic oleophobicity of the Zr:BSA hybrid film toward *n*-hexadecane also remained almost unchanged even after curing, while mobility of *n*-hexadecane drops was inferior and became worsened on the Zr:LSA hybrid film surface after curing at 150 °C for 1 h (substrate TAs increased from 11.4° to 14.2°).

Table 2. Static (θ_S) and Dynamic Dewettability (θ_A/θ_R, $\Delta\theta$, $\Delta\theta_{cos}$, and Substrate TA) of *n*-Hexadecane Droplets on Zr:BSA and Zr:LSA Hybrid Films

curing conditions (temperature and duration)		hardness (GPa)	θ_A/θ_R (°)	$\Delta\theta$ (°)	$\Delta\theta_{cos}$ (−)	TA (°)
Zr:BSA Hybrid Film						
100 °C	1 h	1.95	26.0/21.1	4.9	0.034	10.4
100 °C	24 h	2.27	24.0/17.4	6.6	0.040	10.8
150 °C	1 h	2.37	23.7/18.0	5.7	0.035	11.5
150 °C	24 h	2.20	22.3/15.4	6.9	0.039	10.9
200 °C	1 h	3.03	21.5/15.0	6.5	0.036	9.0
200 °C	24 h	n/a	n/a	n/a	n/a	n/a
Zr:LSA Hybrid Film						
100 °C	1 h	0.95	24.9/16.0	8.9	0.054	11.4
100 °C	24 h	1.26	28.6/20.9	7.7	0.056	11.2
150 °C	1 h	1.19	26.9/19.0	7.9	0.054	14.2
150 °C	24 h	n/a	n/a	n/a	n/a	n/a

Thermoresponsive Properties of Hybrid Films. We further investigated the thermoresponsive properties of our hybrid films. As previously reported, a substantial increase in dynamic dewettability was observed on similar ZrO_2-based hybrid films containing LSA molecules by moderate heating of the surfaces.[35] This increase in dynamic dewettability was attributed to a thermally induced increase in the mobility of functional groups in the surface-tethered molecules causing the liquid-like nature of the surface to further increase. The result was an additional decrease in the energy barriers between metastable states on the high-temperature surfaces, leading to lower resistance to probe liquid droplet motion and significantly improved droplet mobility.[5,35] Actually, Zr:LSA hybrid films (cured at 100 °C for 1 h) exhibited significant reduction in substrate TAs for *n*-hexadecane (from 11.4° to 5.0°) by moderate heating from 25 °C to 70 °C, demonstrating that the Zr:LSA hybrid film surface exhibits thermoresponsive dynamic dewettability. Such thermoresponsive properties were similarly observed for the hybrid films cured under different conditions.

Zr:BSA hybrid films also exhibited significant thermoresponsive dewettability at elevated substrate temperatures, despite it being statically oleophilic! Because of heating of the hybrid film (cured at 100 °C for 1 h), substrate TAs for *n*-hexadecane were reduced from 10.4° (θ_A/θ_R = 26.0°/21.1°, and $\Delta\theta_{cos}$ = 0.034) at 25 °C, to 4.2° (θ_A/θ_R = 16.1°/9.3°, and $\Delta\theta_{cos}$ = 0.026) at 70 °C (see Supporting Information, Movie S-4). Because of the decrease in surface tension of *n*-hexadecane by moderate heating, the dynamic CAs (θ_A/θ_R) decreased markedly. In contrast, $\Delta\theta_{cos}$ and substrate TAs decreased considerably, even though there was a decrease in dynamic CAs. Thus, again, we believe that thermally increased mobility of functional groups in the surface-tethered molecules is considered to be a prime cause for such a thermoresponsive property, similar to our previous paper.[5] These results provide further evidence that the dynamic oleophobicity is controllable through simple adaptation of the physical nature (solidlike or liquid-like) of surface-tethered molecules.

Hydrolytic Stability of Hybrid Films. It is well-known that alkyl carboxylic acid self-assembled monolayers (SAMs) on metal oxide surfaces (alumina, sapphire, and titania) are continuously lost through molecular desorption from the surfaces in an aqueous environment by hydrolytic damage.[43−45] Lim et al. previously reported that serious degradation of the stearic acid-SAMs induced by hydrolytic attack rapidly proceeded within the first 1 h.[43] Such instability of stearic acid-SAMs on metal oxide surfaces in water is a shortcoming of such materials that significantly restricts any potential application. In the present case, similar hydrolytic degradation of the interfacial carboxylate bonding is readily predictable.

Changes in water CAs of our hybrid films (cured at 100 °C for 1 h), as a function of submersion time in hot Milli-Q water (90 °C), are shown in Figure 4. In the case of the Zr:LSA hybrid film, the θ_A values and θ_R values rapidly decreased within the first 5 min (decreased from 111.0° to 89.1° and 93.6° to 11.4°, respectively). While θ_A values decreased slowly with increasing immersion time, the θ_R values reach 0° after only 25 min of immersion. The final θ_A and θ_R values were 40.3°/0.0°, respectively, after 60 min of immersion (those for *n*-hexadecane were 4.4° and 0.0°, respectively). On the other hand, for the Zr:BSA hybrid films, there was an initial drop in both θ_A and θ_R values (decreased from 106.8° to 100.7° and 77.6° to 60.9°,

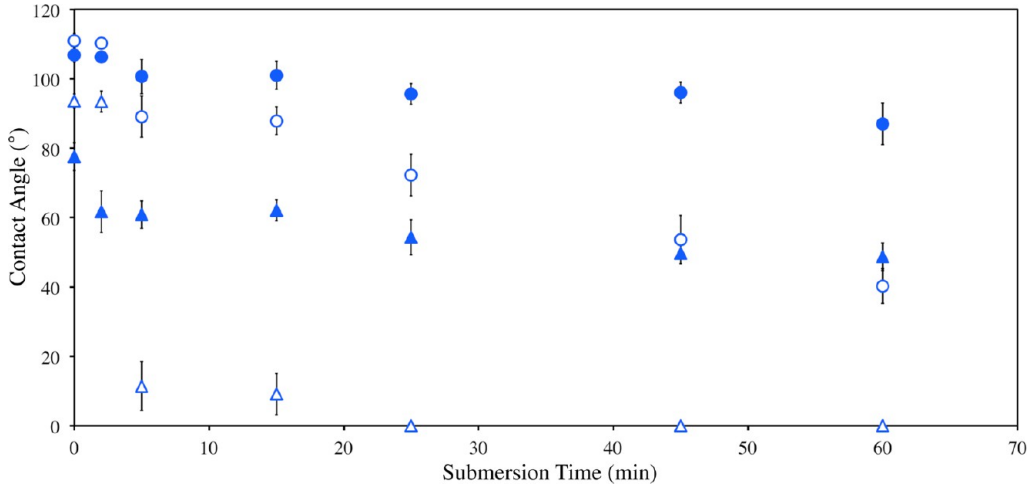

Figure 4. Changes in advancing (θ_A) and receding (θ_R) CAs for water as a function of submersion time in hot water (90 °C). Solid circles and triangles indicate θ_A and θ_R of Zr:BSA, respectively, and open circles and triangles indicate θ_A and θ_R of Zr:LSA, respectively.

respectively) within the first 5 min, and then they gradually diminished as immersion was extended up to 60 min. The final θ_A and θ_R values were 87.2° and 48.7°, respectively (those for *n*-hexadecane were 19.8° and 7.2°, respectively; substrate TA = 12.7°).

This rapid decrease in the θ_A/θ_R values for the Zr:LSA hybrid film clearly indicate that penetration of water had occurred, resulting in hydrolysis of the metal–ligand bond.[43,44] Quick dissociation of the carboxylic acid from the hybrid film surface must lead to a rapid reduction in dewetting properties. In contrast, Zr:BSA hybrid films showed reasonable hydrolytic stability even in hot water. Despite slight decreases in θ_A/θ_R values within the first 5 min, the surfaces retained their hydrophobicity/dynamic oleophobicity, even after submersion was extended to 60 min. Significant increase in hydrolytic stability was observed, compared to the Zr:LSA hybrid film. One of the authors has reported previously that the functional groups of a branched-featured monolayer functioned as a freely rotating umbrella, creating liquid-like surface properties,[46] as well as effectively protecting the metal–ligand bond from hydrolytic attack. This leads to excellent hydrolytic stability in hot water. The BSA molecules may have provided similar protection here.

Antifingerprint Property of Hybrid Films. Besides exceptional transparency, hardness, thermal stability, and hydrolytic stability, we found that our Zr:BSA hybrid films also possess excellent antifingerprint properties. As shown in Figure 5, bare glass slide surfaces exhibited stronger retention of fluorescent fingerprint powders (Figure 5c) than Zr:BSA hybrid film surfaces (cured at 100 °C for 1 h) after application of a fingerprint (Figure 5a). This clearly indicates that fingerprints on the latter surface are less adhered than that on the former surface. Fingerprints on Zr:BSA hybrid films were easily removed by simple washing in flowing water for a few seconds (Figure 5b), while fingerprints stubbornly remained on the bare glass slide (Figure 5d). Low surface energies of SAs may have substantial influence on the excellent antifingerprint property of our hybrid films. However, at present, it is difficult to identify the mechanism of this excellent antifingerprint property of our hybrid surfaces, because the fingerprints are a mixture of water, salts, proteins, oils, and other materials. Therefore, stating that surface energy alone causes this property would be incorrect. We believe that the excellent dynamic oil repellent nature of our films also partially contributes to this property and the actual mechanism is now under investigation. This unique surface property will introduce the potential of Zr:BSA hybrid films for practical applications on optical components, touchscreen devices, and protecting food packages from staining.

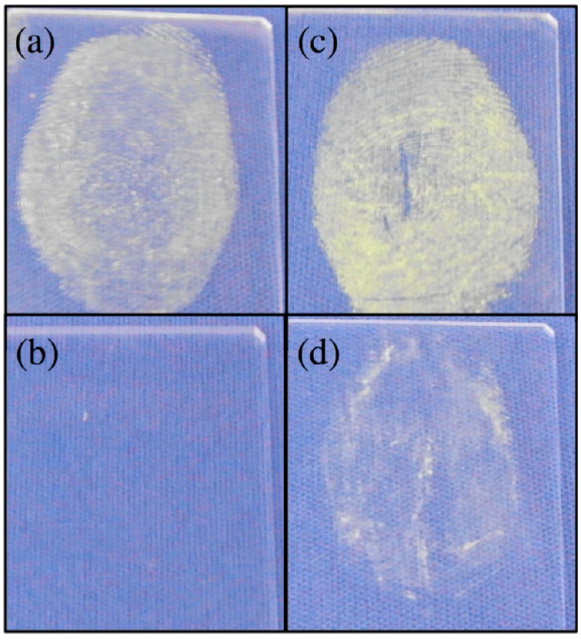

Figure 5. Images of fingerprints detected with yellow fluorescent fingerprint powder on Zr:BSA hybrid films (a) before and (b) after washing with water, respectively. Also pictured are fingerprints on an uncoated glass slide (c) before and (d) after washing with water, respectively.

CONCLUSIONS

We have successfully developed a facile strategy to fabricate smooth, transparent, and hard zirconia (ZrO_2)-based stearic acid (SA) hybrid films showing excellent thermal stability, dynamic/thermoresponsive oleophobicity, and hydrolytic stability. Our experimental results offer clear proof that the molecular architecture (linear or branched) of SA is a key factor in determining the final surface physical/chemical properties of the hybrid films. By selecting a highly branched SA isomer and appropriate preparation conditions, we have successfully overcome many serious shortcomings previously reported for oleophobic films. First, the thermal stability of the hybrid films improved considerably and their dynamic oleophobicity remained almost intact even after being heated to 200 °C for 1 h. Second, since the hybrid films comprised fully cross-linked Zr–O–Zr networks under such a high curing temperature, they also demonstrated reasonable film hardness (3.03 GPa), compared with that of hybrid films prepared with linear-SA (1.19 GPa). Finally, the molecular architecture of SA also generated significant differences in the resistance to the hydrolytic attack in an aqueous environment, since, unlike the linear-functional groups, the branched-functional groups are expected to work as an umbrella and rotate freely. Thus, they effectively shielded and protected the interfacial metal–ligand bond from hydrolytic attack, resulting in its considerable stability, even in hot water (up to 60 min at 90 °C). In addition, the high flexibility of the branched functional groups also increased the ease of *n*-hexadecane droplet motion on the surface. Substrate TAs for a small-volume (5 μL) droplet of *n*-hexadecane markedly decreased from 10.4° to 4.2° by moderate heating of the surface at 70 °C. Moreover, this hybrid film surface was found to display antifingerprint properties that arise, in part, from this excellent dynamic oleophobicity.

Our one-pot coating system reported here is simple, widely reproducible, and allows for the preparation of transparent dynamically oleophobic surfaces over large areas under ambient conditions. Such characteristics of our technique would be ideal for practical applications. This work provides a novel, facile alternative to conventional methods for the fabrication of superoleophobic surfaces, highlighting that neither surface roughening nor perfluorination is necessary. Our technique undoubtedly shows great potential for application in several critical areas, including optical components, touchscreen devices, internal engine/pump coatings, and food packages.

■ ASSOCIATED CONTENT

Supporting Information

Further information on the transparency, as well as movies showing *n*-hexadecane dewetting a Zr:BSA hybrid film surface before and after heating to 70 °C are available in the Supporting Information. This information is available free of charge via the Internet at http://pubs.acs.org/.

■ AUTHOR INFORMATION

Corresponding Author

*E-mail: a.hozumi@aist.go.jp.

Notes

The authors declare no competing financial interest.

■ ACKNOWLEDGMENTS

This work was partially supported by a Grant-in-Aid for Scientific Research on Innovative Areas (A.H. and C.U.; No. 24120005) and Research Activity Start-up (C.U.; No. 23850020) of The Ministry of Education, Culture, Sports, Science, and Technology (MEXT), Japan.

■ REFERENCES

(1) Tuteja, A.; Choi, W.; Ma, M.; Mabry, J. M.; Mazzella, S. A.; Rutledge, G. C.; McKinley, G. H.; Cohen, R. E. *Science* **2007**, *318*, 1618−1622.

(2) Tuteja, A.; Choi, W.; Mabry, J. M.; McKinley, G. H.; Cohen, R. E. *Proc. Natl. Acad. Sci. U.S.A.* **2008**, *105*, 18200−181205.

(3) Wong, T. S.; Kang, S. H.; Tang, S. K. Y.; Smythe, E.; Hatton, B. D.; Grinthal, A.; Aizenberg, J. *Nature* **2011**, *477*, 443−447.

(4) Zhang, J.; Seeger, S. *Angew. Chem., Int. Ed.* **2011**, *50*, 6652−6656.

(5) Cheng, D. F.; Urata, C.; Yagihashi, M.; Hozumi, A. *Angew. Chem., Int. Ed.* **2012**, *51*, 2956−2959.

(6) Deng, X.; Mammen, L.; Butt, H. J.; Vollmer, D. *Science* **2012**, *335*, 67−70.

(7) Cheng, D. F.; Urata, C.; Masheder, B.; Hozumi, A. *J. Am. Chem. Soc.* **2012**, *134*, 10191−10199.

(8) Kota, A. K.; Li, Y. X.; Mabry, J. M.; Tuteja, A. *Adv. Mater.* **2012**, *24*, 5838−5843.

(9) Park, J.; Urata, C.; Masheder, B.; Dalton F. Cheng, D. F.; Hozumi, A. *Green Chem.* **2013**, *15*, 100−104.

(10) Callies, M.; Quere, D. *Soft Matter* **2005**, *1*, 55−61.

(11) Quere, D. *Rep. Prog. Phys.* **2005**, *68*, 2495−2532.

(12) Jung, Y. C.; Bhushan, B. *ACS Nano* **2009**, *3*, 4155−4163.

(13) Bhushan, B.; Jung, Y. C. *Prog. Mater. Sci.* **2011**, *56*, 1−108.

(14) Xu, L.; Karunakaran, R. G.; Guo, J.; Yang, S. *ACS Appl. Mater. Interfaces* **2012**, *4*, 1118−1125.

(15) Chen, Y.; Zhang, Y.; Shi, L.; Li, J.; Xin, Y.; Yang, T.; Guo, Z. *Appl. Phys. Lett.* **2012**, *101*, 033701−033701−4.

(16) Wu, T.; Suzuki, Y. *Sens. Actuators, B* **2011**, *156*, 401−409.

(17) Kota, A. K.; Choi, W.; Tuteja, A. *MRS Bull.* **2013**, *38*, 383−390.

(18) Butt, H.-J.; Semprebon, C.; Papadoloulos, P.; Vollmer, D.; Brinkmann, M.; Ciccotti, M. *Soft Matter* **2013**, *9*, 418−428.

(19) Leng, B. X.; Shao, Z. Z.; de With, G.; Ming, W. H. *Langmuir* **2009**, *25*, 2456−2460.

(20) Darmanin, T.; Guittard, F.; Amigoni, S.; de Givenchy, E. T.; Noblin, X.; Kofman, R.; Celestini, F. *Soft Matter* **2011**, *7*, 1053−1057.

(21) Verho, T.; Bower, C.; Andrew, P.; Franssila, S.; Ikkala, I.; Ras, R. H. A. *Adv. Mater.* **2011**, *23*, 673−678.

(22) Zushi, Y.; Hogarh, J. N.; Masunaga, S. *Clean Technol. Environ. Policy* **2011**, *14*, 9−20.

(23) Lindstrom, A. B.; Strynar, M. J.; Libelo, E. L. *Environ. Sci. Technol.* **2011**, *45*, 7954−7961.

(24) Ma, W.; Higaki, Y.; Otsuka, H.; Takahara, A. *Chem. Commun.* **2013**, *49*, 597−599.

(25) Fadeev, A. Y.; McCarthy, T. J. *Langmuir* **1999**, *15*, 7238−7243.

(26) Chen, W.; Fadeev, A. Y.; Hsieh, M. C.; Oner, D.; Youngblood, J.; McCarthy, T. J. *Langmuir* **1999**, *15*, 3395−3399.

(27) Fadeev, A. Y.; McCarthy, T. J. *Langmuir* **1999**, *15*, 3759−3766.

(28) Hozumi, A.; Cheng, D. F.; Yagihashi, M. *J. Colloid Interface Sci.* **2011**, *353*, 582−587.

(29) Krumpfer, J. W.; McCarthy, T. J. *Faraday Discuss.* **2010**, *146*, 103−110.

(30) Urata, C.; Masheder, B.; Cheng, D. F.; Hozumi, A. *Chem. Commun.* **2013**, *49*, 3318−3320.

(31) Urata, C.; Masheder, B.; Cheng, D. F.; Hozumi, A. *Langmuir* **2012**, *28*, 17681−17689.

(32) Bikerman, J. J. *J. Phys. Colloid Chem.* **1950**, *54*, 653−658.

(33) Good, R. J. *J. Am. Chem. Soc.* **1952**, *74*, 5041−5042.

(34) Schwartz, A. M.; Minor, F. W. *J. Colloid Sci.* **1959**, *14*, 584−597.

(35) Masheder, B.; Urata, C.; Cheng, D. F.; Hozumi, A. *ACS Appl. Mater. Interfaces* **2013**, *5*, 154−163.

(36) Kemnitz, C. R.; Mackey, J. L.; Loewen, M. J.; Hargrove, J. L.; Lewis, J. L.; Hawkins, W. E.; Nielsen, A. F. *Chem.—Eur. J.* **2010**, *16*, 6942−6949.

(37) Spiegel, A.; Bruenger, W. H.; Dzionk, C.; Schmuki, P. *Microelectron. Eng.* **2003**, *67*−*68*, 175−181.

(38) Hidber, P. C.; Helbig, W.; Kim, E.; Whitesides, G. M. *Langmuir* **1996**, *12*, 1375−1380.

(39) Honda, K.; Morita, M.; Otsuka, H.; Takahara, A. *Macromolecules* **2005**, *38*, 5699−5705.

(40) Honda, K.; Morita, M.; Sakata, O.; Sasaki, S.; Takahara, A. *Macromolecules* **2010**, *43*, 454−460.

(41) Lucca, D. A.; Klopfstein, M.; Ghisleni, R.; Gude, A.; Mehner, A.; Datchary, W. *CIRP Ann.-Manuf. Tech.* **2004**, *53*, 475−478.

(42) Kessman, A. J.; Huckaby, D. K. P.; Snyder, C. R.; Kukureka, S. N.; Cairns, D. R. *Wear* **2009**, *267*, 614−618.

(43) Lim, M. S.; Feng, K.; Chen, X. Q.; Wu, N. Q.; Raman, A.; Nightingale, J.; Gawalt, E. S.; Korakakis, D.; Hornak, L. A.; Timperman, A. T. *Langmuir* **2007**, *23*, 2444−2452.

(44) Liakos, I. L.; Newman, R. C.; McAlpine, E.; Alexander, M. R. *Langmuir* **2007**, *23*, 995−999.

(45) Lim, J.; Kwon, Y. S.; Park, S.-H.; Song, I. Y.; Choi, J.; Park, T. *Langmuir* **2011**, *27*, 14647−14653.

(46) Hozumi, A.; McCarthy, T. J. *Langmuir* **2010**, *26*, 2567−2573.